Modeling and Analysis

GREENHOUSE GASES SCIENCE AND TECHNOLOGY

Underground CO_2 storage: demonstrating regulatory conformance by convergence of history-matched modeled and observed CO_2 plume behavior using Sleipner time-lapse seismics

R. Andrew Chadwick and David J. Noy, British Geological Survey, Keyworth, Nottingham, UK

Abstract: One of the three key regulatory requirements in Europe for transfer of storage site liability is to demonstrate conformity between predictive models of reservoir performance and monitoring observations. This is a challenging requirement because a perfect and unique match between observed and modeled behavior is near impossible to achieve. This study takes the time-lapse seismic monitoring data from the Sleipner storage operation to demonstrate that as more seismic data becomes available with time, predictive models can be matched more accurately to observations and become more reliable predictors of future performance. Six simple performance measures were defined: plume footprint area, maximum lateral migration distance of CO_2 from the injection point, area of CO_2 accumulation trapped at top reservoir, volume of CO_2 accumulation trapped at top reservoir, area of all CO_2 layers summed, and spreading co-efficient. Model scenarios were developed to predict plume migration up to 2008. Scenarios were developed for 1996 (baseline), 2001, and 2006 conditions, with models constrained by the information available at those times, and compared with monitoring datasets obtained up to 2008. The 1996 predictive range did generally encompass the future observed plume behavior, but with such a wide range of uncertainty as to render it of only marginal practical use. The 2001 predictions (which used the 1999 and 2001 seismic monitoring datasets) had a much lower uncertainty range, with the 2006 uncertainties somewhat lower again. There are still deficiencies in the actual quality of match but a robust convergence, with time, of predicted and observed models is clearly demonstrated. We propose modeling-monitoring convergence as a generic approach to demonstrating conformance. © 2015 Society of Chemical Industry and John Wiley & Sons, Ltd

Keywords: CO_2 storage; monitoring and verification; Sleipner; CCS; time-lapse seismic; conformance

Correspondence to: R. Andrew Chadwick. E-mail: rach@bgs.ac.uk

Received December 10, 2014; revised February 12, 2015; accepted February 13, 2015
Published online at Wiley Online Library (wileyonlinelibrary.com). DOI: 10.1002/ghg.1488

Introduction

Conformance is a measure of how well a product or system meets a specified standard and is a key requirement for storage under European CCS regulation.[1] To demonstrate conformance, a storage site operator must show agreement between predictive models of reservoir performance and monitoring observations. Conformance indicates that storage processes are well understood and increases the likelihood of longer-term predictions being reliable. Satisfactory conformance is required through the operational phase and, crucially, at the end of this, for the transfer of responsibility for the site from the operator to the national authority.

Demonstrating conformance is challenging because a perfect and unique match between observed and modeled behavior is to all intents and purposes impossible, due to limitations in geological understanding, modeling software and resolution of the monitoring tools. The aim of this paper is to show that conformance can be demonstrated by showing that predictive modeling capability increases systematically with time as monitoring data is progressively acquired.

We use the time-lapse monitoring datasets acquired during the Sleipner CO_2 storage operation to show how predictive modeling improves as more monitoring data is acquired, and, as a direct consequence, unexpected or divergent future outcomes become increasingly unlikely.

Sleipner summary

The Sleipner gas fields are located in the Norwegian sector of the North Sea operated by Statoil and partners (Fig. 1(a)). Natural gas from the Sleipner West Field has a CO_2 content of between 4 and 9.5% which has to be reduced below 2.5%, prior to delivery into the European gas supply network. CO_2 is removed from the natural gas on the platform and, in response to the Norwegian offshore carbon tax, is injected into the Utsira Sand, a regional scale saline aquifer. [2,3]

Summary site geology

The geological setting of Sleipner is relatively simple. Details are set out in a number of publications [4,5] and only a brief summary is given here.

The Sleipner storage reservoir is the Utsira Sand, a saline aquifer of Mio-Pliocene age and of regional extent, stretching more than 400 km north to south and between 50 and 100 km east to west. Around Sleipner, the top reservoir surface is around 800 m deep and the reservoir is about 250 m thick. In the immediate vicinity of Sleipner detailed mapping from 3D seismic data shows the top of the reservoir to be gently undulatory with small domes and valleys (Fig. 2(a)).

Reservoir and overburden properties

The Utsira Sand comprises stacked overlapping 'mounds' of very low relief, interpreted as individual

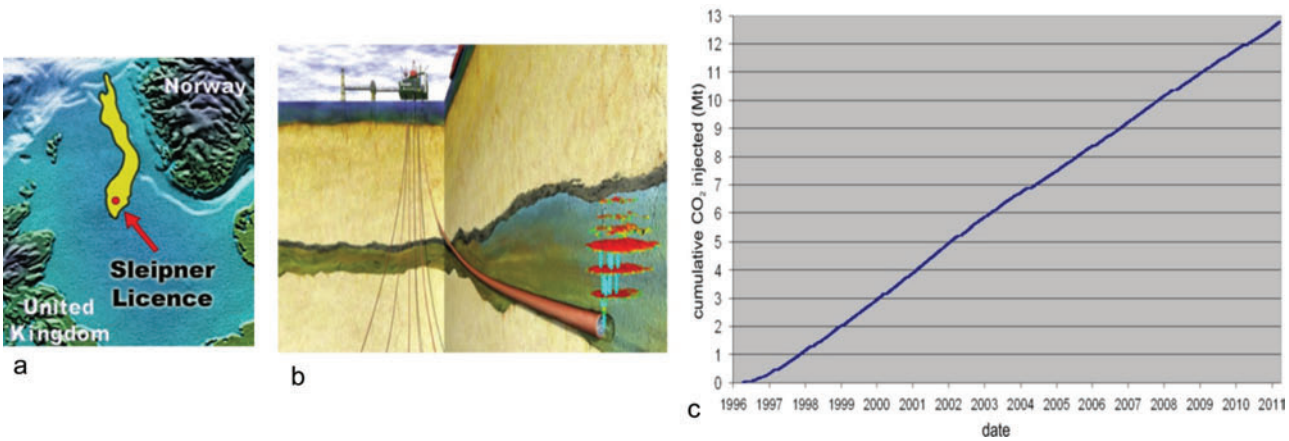

Figure 1. (a) Regional location map of Sleipner and the Utsira Sand (yellow polygon); (b) Schematic diagram of the Sleipner injection infrastructure and the CO_2 plume; (c) Sleipner cumulative CO_2 injected amount over time. (Sleipner map and schematic courtesy of Statoil ASA.)

 Greenhouse Gases: Science and Technology published by Society of Chemical Industry and John Wiley & Sons, Ltd. | *Greenhouse Gas Sci Technol.* **5**:305–322 (2015); DOI: 10.1002/ghg

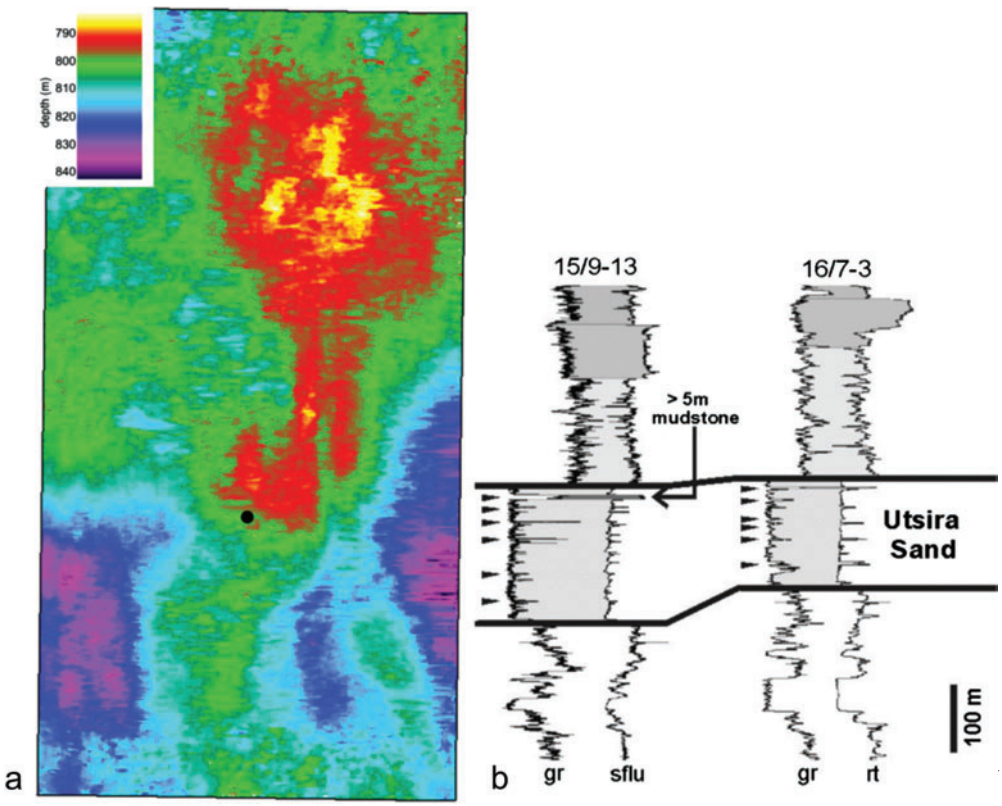

Figure 2. (a) Top reservoir depth map around Sleipner (~7 × 3 km). Black disc denotes location of injection point. (b) Sample geophysical logs through the Utsira Sand from two wells in the Sleipner area. Note the low γ-ray signature of the Utsira Sand, with peaks denoting the intra-reservoir mudstones. gr = γ-ray log, sflu/rt = resistivity logs.

fan-lobes and commonly separated by thin intra-reservoir mudstones. On geophysical logs it characteristically shows a sharp top and base (Fig. 2(b)), with the proportion of clean sand in the reservoir unit varying generally between 0.7 and 1.0. Macroscopic and microscopic analysis of core and cuttings show it to be mostly fine-grained and largely uncemented[4] with porosities in the range 27 to 42%. Permeabilities are high with measured values from core testing ranging between 1 and 3 darcy and, from water production, ranging up to 8 darcy.

The non-sand fraction mostly comprises thin mudstones (typically about 1 m thick), which show as peaks on the gamma-ray and resistivity logs. In the Sleipner area, a thicker mudstone, some 5 to 7 m thick separates the uppermost sand unit from the main reservoir beneath. The mudstone layers constitute important permeability barriers within the reservoir sand and have a dominant effect on CO_2 migration through the reservoir as evidenced below.

The overburden of the Utsira reservoir around Sleipner is about 700 m thick and dominantly argillaceous. The immediate topseal is a laterally persistent silty mudstone some 50 to 100 m thick, extending more than 50 km west and 40 km east of the area currently occupied by the injected CO_2 and well beyond the predicted final migration distance of the projected total injected volume.[6] Laboratory gas transport testing on a core sample obtained from this unit shows it to be a very low permeability capillary seal.[7]

Injection profile

The Sleipner CO_2 injection point is positioned beneath a small domal feature in the topseal that rises about 12 m above the surrounding area (Fig. 2 (a)). The aim was to minimize the lateral spread of the plume at the reservoir top and reduce the spatial footprint of any monitoring that might be required, particularly in the early stages of the project.

Injection, at around 1 Mt per year, is via a single deviated well, sub-horizontal at the injection point with the wellbore lying beneath the buoyant plume (Figs. 1(b) and 1(c)). This is important for two reasons. First, the wellbore lies beneath the buoyant CO_2 plume which minimizes the containment risk. Second, no invasive monitoring or direct invasive measurement of the plume is possible.

Monitoring data

The key monitoring dataset at Sleipner comprises time-lapse 3D seismics which provide striking high resolution images of the developing CO_2 plume. [8–10] The time-lapse campaign includes a pre-injection 'baseline' dataset acquired in 1994, followed by repeat surveys in 1999, 2001, 2002, 2004, 2006, and 2008. A subset of the full time-lapse ensemble (Fig. 3) shows

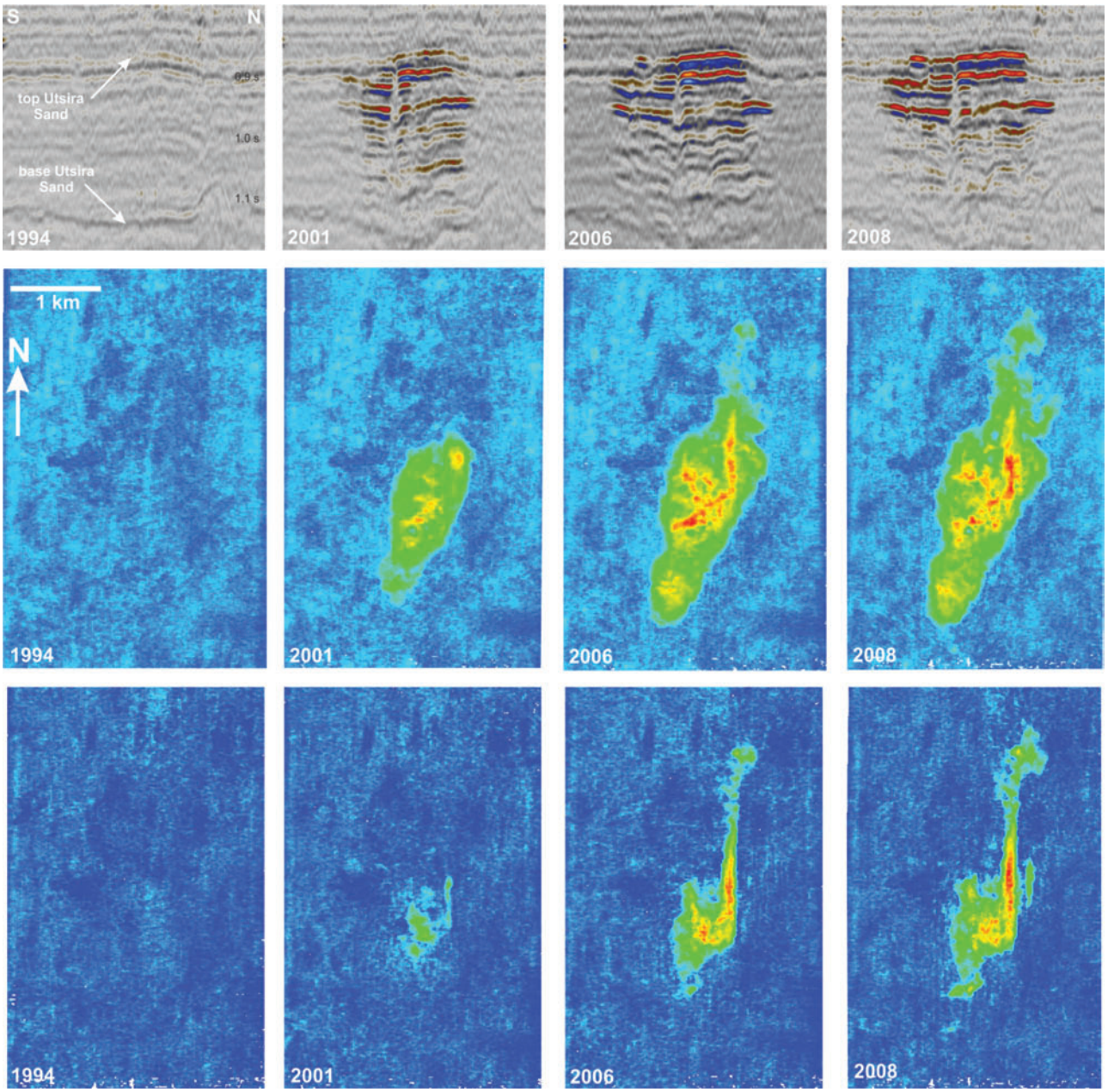

Figure 3. The Sleipner CO_2 plume showing its evolution from 1994 (baseline) to 2008. Top panels show the development of reflectivity on a N-S cross-section (inline), middle panels show maps of the whole plume reflectivity footprint, bottom panels show maps of the reflectivity of the topmost CO_2 layer.

the CO_2 plume as a tiered feature, roughly 200 m high and elliptical in plan, with a major axis approaching 4000 m by 2008 and comprising a number of bright sub-horizontal reflections within the reservoir, growing with time. Interpretations of the plume reflectivity [9,10] identified nine separate reflective levels in the reservoir which correspond to trapped CO_2. These individual and interpretatively distinct reflections have remained consistently identifiable from the first time-lapse survey in 1999 to the most recent, and are interpreted as corresponding to thin layers of CO_2 trapped beneath thin intra-reservoir mudstones and the reservoir topseal. The detectability limit, at the outer edge of the layers, is reckoned to be around 1 m thickness or less.[11]

Demonstrating conformance

It is clear from the storage literature that exact history-matching between predictive models and flow simulation is very difficult to achieve, even where reservoir processes are otherwise well understood, and this has also been the case at Sleipner.[11,12] An alternative way of indicating conformance is to show that predictive modeling capability improves progressively as more monitoring data becomes available. This shows that the geological model and modeling assumptions are basically robust and additional data lead to progressive model improvement and refinement, rather than triggering radical model modifications.

The aim in this paper is to use the Sleipner site characterization and monitoring datasets to assess the level of agreement between predictive reservoir flow models of storage performance and monitoring observations and how this has evolved through time as more monitoring data has become available and understanding of storage processes has improved.

Methodology

In order to evaluate the development of conformance through time, we reconstruct the operational history of Sleipner retrospectively, starting with predictions based on baseline information only, but moving forward through time and progressively improving predictive models as more monitoring data became available (Fig. 4). Thus, the initial set of predictive models was constructed for 1996, just prior to injection start-up, and utilizing the datasets that were available at that time (essentially the baseline and legacy datasets). The second set of predictive models was constructed for 2001 utilizing the 1999 and 2001 time-lapse seismic datasets and the final set of predictive models was constructed for 2006 utilizing the 2004 and 2006 time-lapse datasets plus additional reservoir temperature information.

The principle of the analysis is to compare the predictive models with subsequent monitoring data to assess the degree of conformance (i.e., the match between the prediction and the observation) and how this has changed through time (Fig. 4). In order to do this a set of quantifiable performance measures was defined such that predictions could be objectively compared with observations.

Performance measures

The time-lapse seismics define a robust plume geometry that evolves systematically with time and from this, six readily measurable key performance measures were defined:

Plume footprint area is the basic measure of plume spreading and migration showing the reservoir area being impacted by free CO_2.

Maximum lateral migration distance of CO_2 from the injection point gives a first order estimate of plume mobility and the propensity of the plume to move rapidly away from the injection well towards, for example, potential spill-points.

Area of CO_2 accumulation trapped at top reservoir provides a first order indication of the ease with which CO_2 migrates upwards through the reservoir, and the storage potential of the reservoir itself. In the longer-term most of the injected CO_2 at Sleipner will accumulate at the reservoir top, so analysis of the topmost accumulation proves a pointer to the longer-term behavior of the plume.

Volume of CO_2 accumulation trapped at top reservoir gives a more robust indication of CO_2 migration up through the reservoir. It is however quite difficult to quantify. Here we use up to three different estimates of top layer volume derived from the time-lapse seismics.[11]

Area of all CO_2 layers summed provides an indication of how much CO_2 is being trapped at various levels within the reservoir and a measure of the lateral dispersion of CO_2 within the reservoir.

Spreading co-efficient is defined as the plume footprint area divided by the area of all the layers summed. It gives a measure of the storage efficiency of

	1994	1995	1996	1997	1998	1999	2000	2001	2002	2003	2004	2005	2006	2007	2008	2009	2010	2050	2100	2200
3D surface seismic																				
Baseline prediction																				
2001 prediction																				
2006 prediction																				
Cumulative CO_2 injected at TL seismic surveys (Mt)	0.00		injection starts			2.35		4.25	4.97		6.84	7.74	8.40		10.15					

a

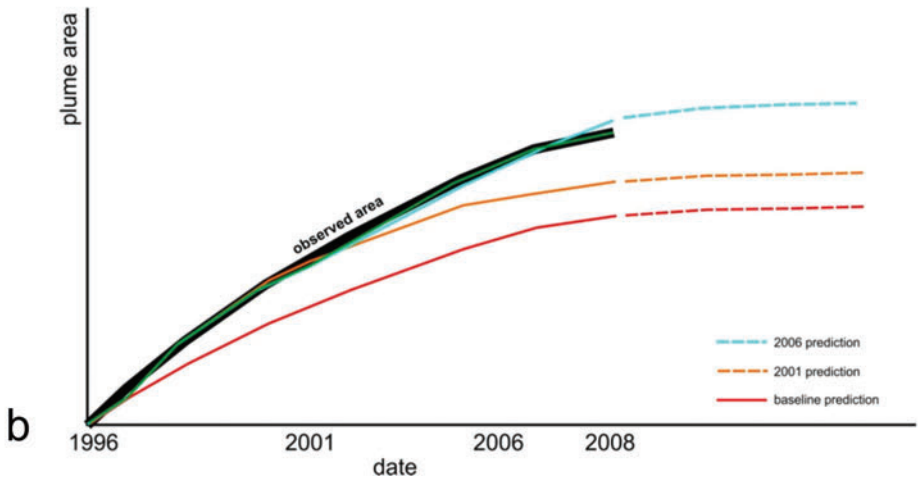

Figure 4. Time-lapse 3D seismic monitoring schedule, in relation to the reconstructed predictive sequences (a); Schematic representation of the retrospective predictive modeling concept showing predictions based on 1996, 2001, and 2006 datasets compared with an observed performance measure (in this case plume area), with degree of conformance improving with time (b).

the reservoir during the injection phase. A value of unity corresponds to all of the CO_2 in a single layer and low storage efficiency; lower values indicate partition of CO_2 into multiple layers with greater storage efficiency.

Modeling strategy

The modeling strategy was to build a series of TOUGH2 reservoir flow models [13,14] that reflect the state of knowledge at each of the selected time-steps (1996, 2001, and 2006) and encompass the estimated range of parameter uncertainty at that time. The model predictions were then compared with the monitored values of the performance indicators to assess the degree of conformance and how this changed with time, as more monitoring data were acquired.

The models were kept relatively simple so that the effects of changing specific model parameters could be clearly isolated and also to allow multiple model scenarios to be run in reasonable computer run-times. The basic model geometry was 2D axisymmetric (radial), which is compatible with the flat-lying nature of the Utsira Sand reservoir and with the limited understanding of the fine-scale internal structure of the reservoir in the vicinity of the CO_2 plume (Fig. 5). The model is 215 m high from the injection point to the topseal and contains seven thin mudstones (typically ~1 m thick) with intervening sandstones (typically 16 to 50 m thick). Model layer cell dimensions are 1 to 2 m vertically and horizontally start at 5m at the axis expanding to 30 m between radial distances of 100 m and 1 km with further expansion thereafter reaching 340 m at a radius of 5 km. The emphasis is on reproducing realistic CO_2 lateral migration in the axial part of the model. Including the topseal, the mudstones allow up to eight spreading layers of CO_2 (notionally equivalent to the nine individual CO_2 layers identified on the seismic data, of which one or two are of

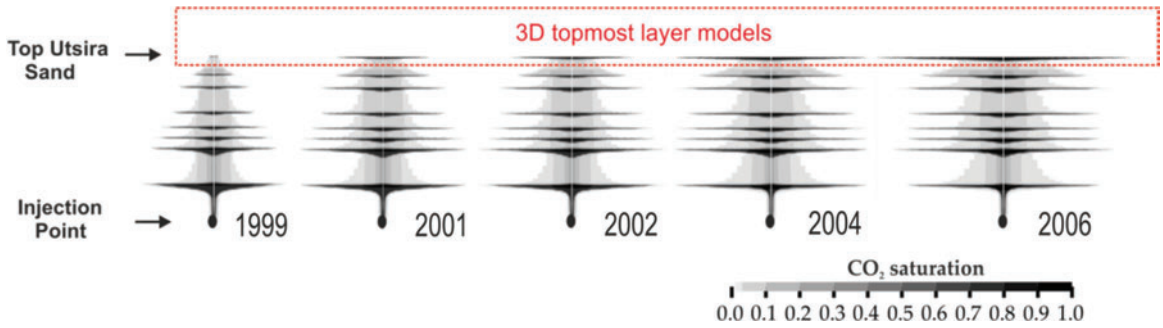

Figure 5. Basic geometry of the TOUGH2 axisymmetric model showing a typical flow simulation for the progressive growth of the CO_2 plume to 2006. Conceptual 3D topmost layer models indicated in red. N.B. In subsequent figures only half of the axisymmetric model is shown.

limited lateral extent). Initial sandstone permeabilities, based on core measurements, are in the range 1–3 Darcy. The mudstones are 'semi-permeable' to reflect either homogeneous low permeability or equivalent impermeable mudstones with many small holes. Permeabilities of the mudstones are empirical, derived from the observed speed of plume development, and vary in the range 70–300 mD. Relative permeability and capillary pressure functions follow experimental results from Utsira Sand core (Erik Lindeberg pers. comm.), with residual saturations for water and CO_2 of 0.05 and zero, respectively. Ambient water flow in the reservoir is assumed to be absent, consistent with near-hydrostatic pressures measured in boreholes scattered regionally across the Utsira Sand.

The topmost CO_2 layer in the plume is the primary determinant of storage performance in the medium and longer term, as a progressively larger proportion of CO_2 will become trapped beneath the topseal with time. To address this, a suite of ancillary 3D models was also built incorporating the topography of the reservoir topseal in order to enable accurate prediction of sub-topseal lateral migration. The 3D models were coupled to the axisymmetric models in being supplied by the modeled CO_2 flux arriving at the base of the uppermost sand layer situated beneath the reservoir topseal.

For the whole study, looking at 1996, 2001, and 2006 prediction scenarios, in excess of 45 axisymmetric models were run, with more than 21 3D models of the topmost layer.

In this paper an illustrative outline of the full conformance study is presented, showing a few key examples of all the model scenarios.

1996 model: predictions based on 1996 baseline datasets

Prior to injection in 1996 only the baseline datasets were available:

- 2D seismic surveys across the full extent of the Utsira Sand and beyond (~16000 line km).
- Local 3D survey in the vicinity of Sleipner (~770 km^2).
- Large numbers (~130) of wells with cuttings and geophysical logs across the extent of the Utsira Sand and beyond.
- Estimates of various physical properties for the reservoir.

Temperature information for the Utsira Sand was rather ambiguous. A single downhole measurement suggested an injection point temperature of 36°C. On the other hand interpolation from temperatures in the deeper gas field suggested a warmer reservoir, about 41°C at the injection point.

For the 1996 scenarios, the principal uncertainty was the nature of the intra-reservoir mudstones, and how efficiently they acted as flow barriers. Permeable (or laterally very impersistent) mudstones would lead to accumulation of a single layer of CO_2 at the top of the reservoir. Conversely, wholly impermeable mudstones would also result in a single layer of CO_2, but beneath the first mudstone above the injection point. Semi-permeable mudstones which retard but do not prevent the passage of CO_2, would promote development of a multi-layer plume. These alternative mudstone scenarios were modeled (Fig. 6).

In some of the modeling runs, sand permeabilities were also varied, between 1 darcy and 3 darcy, as were

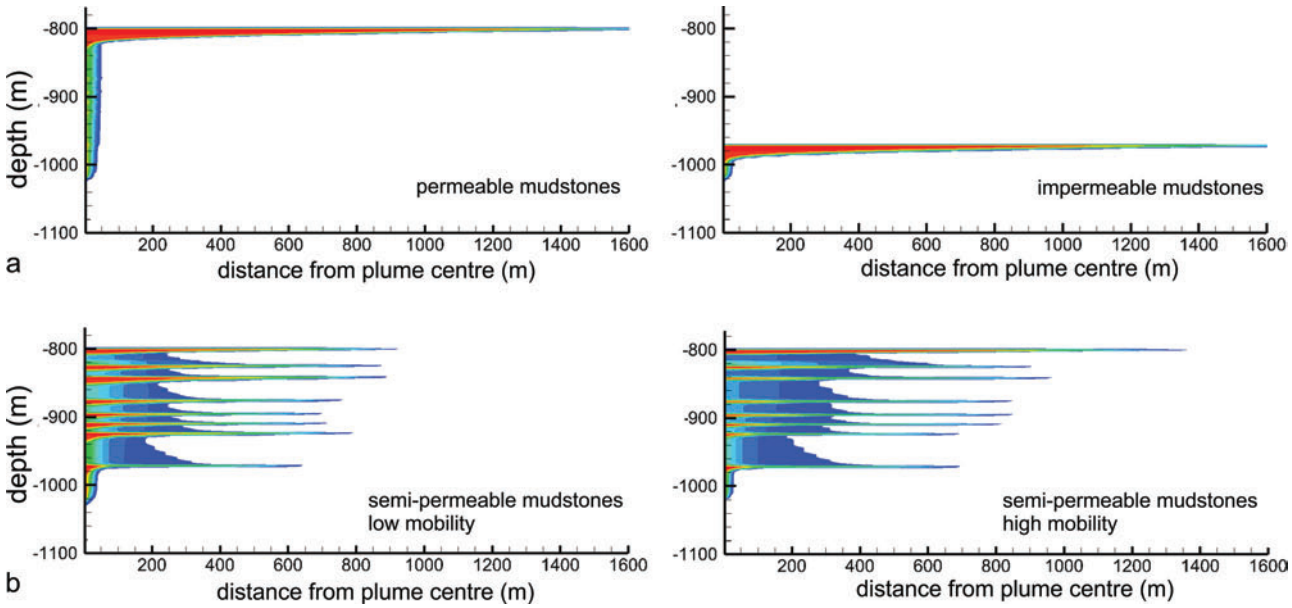

Figure 6. Predicted plume development for 2008 for the multi-layer plume, based on information available in 1996. Permeable and impermeable mudstones lead to single layer plumes (a) and models with semi-permeable mudstones and cool and warm reservoir options leading to multi-layer plumes (b). Note how single layer scenarios give rise to much more lateral spreading than the multi-layer scenario. (Red denotes high CO_2 saturation, blue denotes low CO_2 saturation)

reservoir temperatures, with 'cool' reservoir scenarios (29 °C at the reservoir top, 36 °C at the injection point) and 'warm' reservoir scenarios (33 °C at the reservoir top, 41 °C at the injection point). The warm reservoir / high sand permeability scenarios lead to greater CO_2 mobility (lower viscosity and density) and generally to greater lateral spread than the cool /low permeability scenarios (Fig. 6).

This uncertainty in reservoir properties leads to major variation in the predicted performance measures. For example the predicted plume footprint area by 2008 varies between ~2 km^2 for a multi-layer plume and >7 km^2 for single layer plumes (Fig. 7). The actual values subsequently measured from the seismic time-lapse monitoring lie between the predicted end-members, but are rather similar to the predictions using 'semi-permeable' mudstones. Other investigated reservoir properties such as sand permeability and temperature also have a significant effect on predicted outcomes, though not as fundamentally as do the mudstone properties (Fig. 8).

Another key performance measure is the development of the topmost layer in the CO_2 plume (Fig. 9). Predicted volumes of CO_2 trapped at the reservoir top by 2008 vary from zero (with impermeable intra-reservoir mudstones) to > 12 Mm^3 (wholly permeable mudstones). The subsequently observed values lie within these limits with the semi-permeable mudstone models showing quite a good match to the observed values. The latter is in a sense fortuitous, as no monitoring data were available in 1996 to calibrate the mudstone permeabilities.

Development of the topmost CO_2 layer is driven by two factors: the amount of CO_2 provided to the reservoir top by the axisymmetric models (Fig. 9) and conditions controlling migration of CO_2 beneath the topseal (principally the temperature and permeability of the top reservoir sand). 3D models of the topmost layer therefore show a wide range of development (Fig. 10). One end-member (impermeable intra-reservoir mudstones) allows no CO_2 at all to reach the reservoir top, whereas the other end-member (permeable intra-reservoir mudstones) allows almost all of the injected CO_2 to reach the reservoir top. This level of uncertainty leads to a very wide range of possible outcomes. The observed topmost layer from 2008 (Fig. 10(c)) does fall between the predicted end-members though, so the predictive modeling, even with large uncertainty, is clearly useful in constraining possible outcomes.

| *Greenhouse Gas Sci Technol.* **5**:305–322 (2015); DOI: 10.1002/ghg

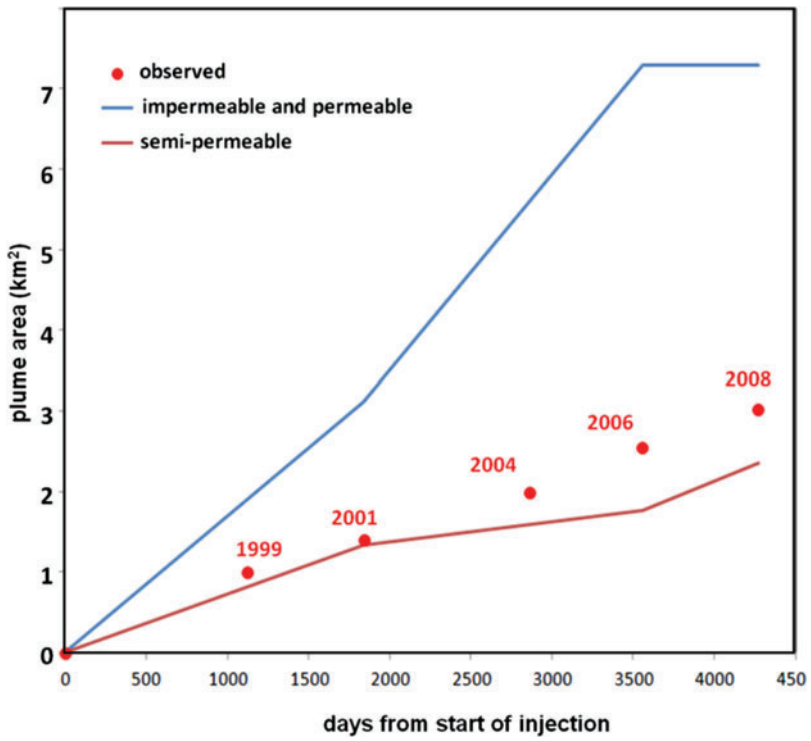

Figure 7. 1996 scenarios showing the effect of intra-reservoir mudstones properties on predicted plume footprint area. Actual values subsequently observed on seismic monitoring data also shown.

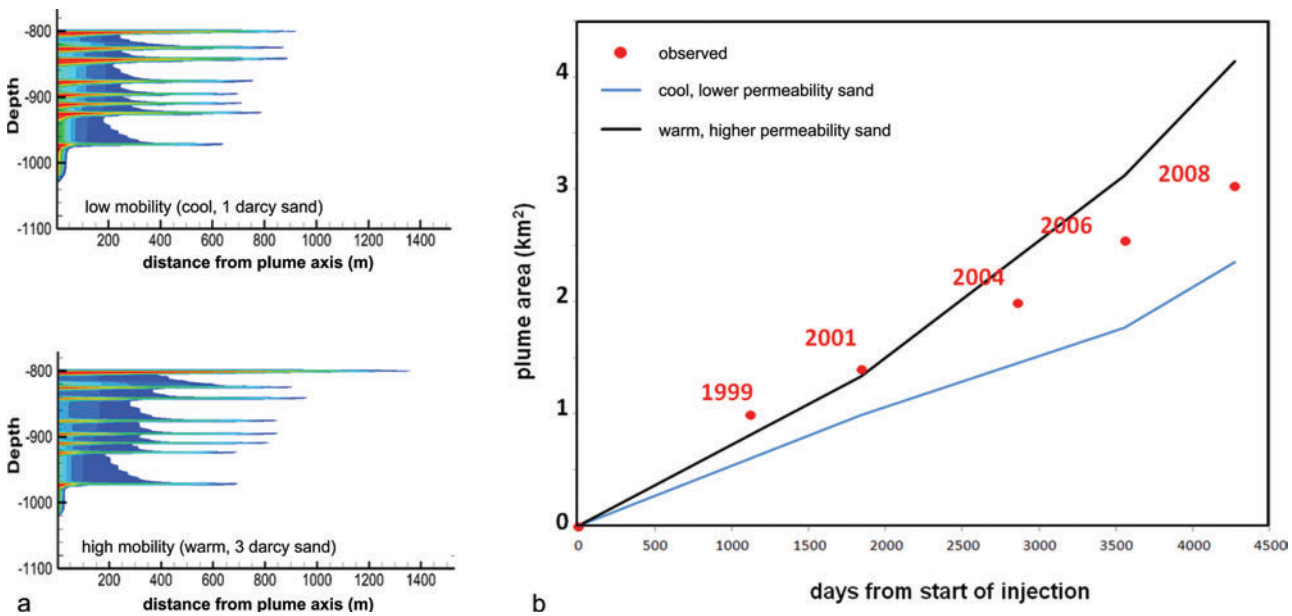

Figure 8. 1996 scenarios showing the effect of sand permeability and reservoir temperature. Predicted plume development in 2008 (a) and predicted plume area end-members compared with subsequent monitoring measurements (b).

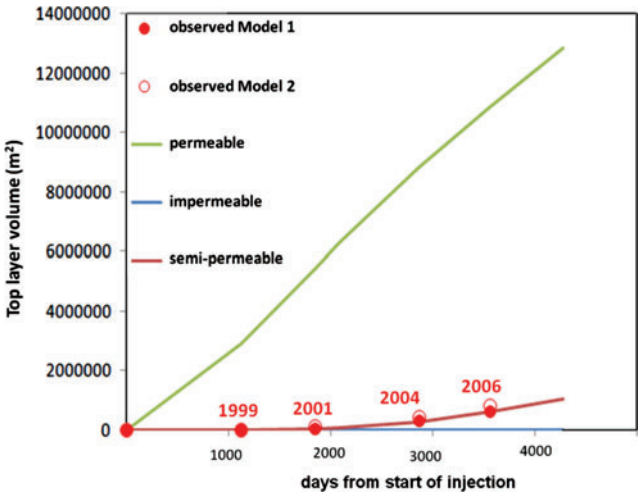

Figure 9. Effect of intra-reservoir mudstones properties on predicted volume of the topmost CO_2 layer, compared with two quantitative estimates (Models 1 and 2) derived from the time-lapse seismic measurements.[11]

Results from all of the modeled scenarios and how they compare with the monitoring observations are summarized below in terms of the end-members which give the 'maximum' and 'minimum' limits of each performance measure (Fig. 11):

The observed ***plume footprint area*** is towards the lower limits of the predicted range. This is because the plume is in fact a multi-layer feature (Fig. 3), so the single layer scenarios tend to markedly overstate plume footprint.

Observed ***lateral migration distance from the injection point*** lies towards the upper limit of the predicted range but is encompassed by the high mobility scenario of the 3D model. The main reason that the predicted migration distances are generally lower than observed is the marked anisotropic nature of the plume spread with its pronounced NNE-SSW elongation (Fig. 3). This was not known until the first monitoring data became available in 1999.

The observed ***area of the CO_2 accumulation trapped at top reservoir*** is significantly lower than the upper limits of both the axisymmetric and the 3D modeled scenarios. That is because the latter both assume a single layer which contains almost the full amount of injected CO_2, the former spreading unfettered beneath a flat topseal, the latter spreading beneath the observed topseal relief. The lower 3D limit corresponds to semi-permeable mudstones, with multiple CO_2 layers and a cool reservoir with low permeability sand which does not allow sufficient CO_2 to reach the reservoir top. The axisymmetric lower limit is the impermeable mudstone scenario which does not allow any CO_2 to reach the reservoir top.

The observed ***volume of the CO_2 accumulation trapped at top reservoir*** is much lower than the upper axisymmetric limit which assumes a single layer with almost all of the injected CO_2 accumulating at the reservoir top. In addition, the warm reservoir scenario maximizes total CO_2 volume. The multiple layer scenarios provide a much better match for this performance measure.

The observed ***area of all layers summed*** falls well within the upper and lower limits of the predicted scenarios.

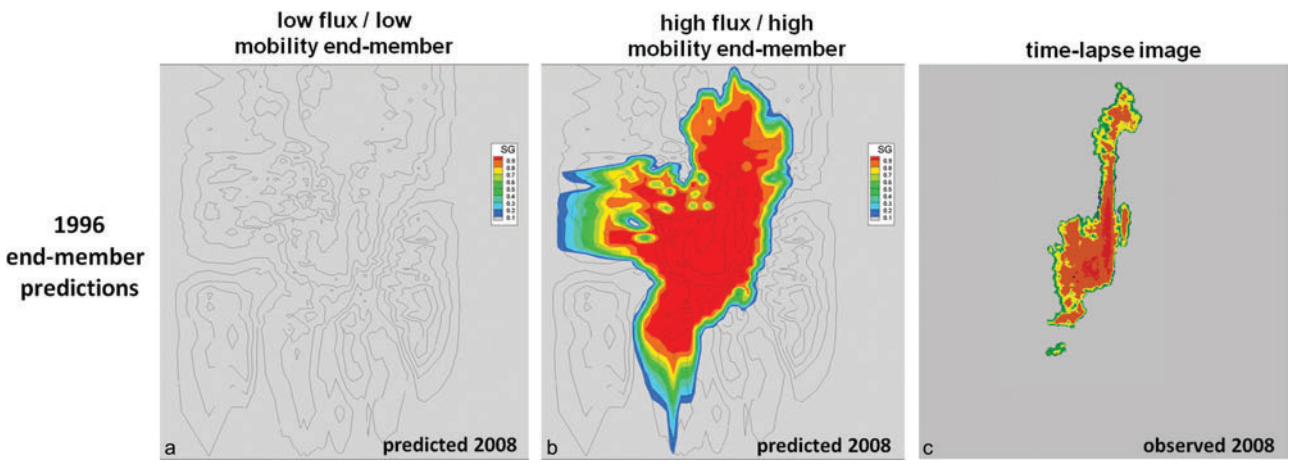

Figure 10. Predictive 3D flow models of topmost layer development by 2008 based on information available in 1996, assuming wholly impermeable intra-reservoir mudstones (a) and wholly permeable mudstones (b), compared with actual monitoring data acquired in 2008 (c).

| *Greenhouse Gas Sci Technol.* **5**:305–322 (2015); DOI: 10.1002/ghg

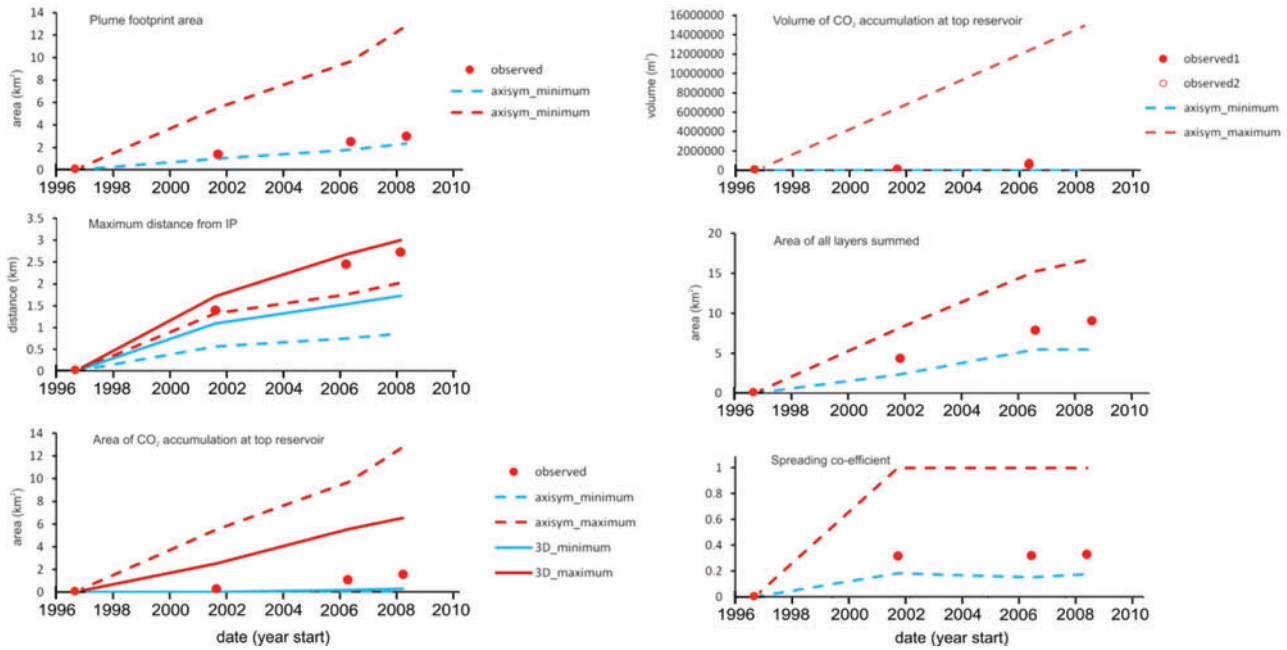

Figure 11. Summary synthesis plots for the performance measures from 1996 showing the minimum and maximum end-members of the model predictions and the observed data (red spots). Topmost layer volumes are estimated from the seismic data using two different methods.[11]

The observed ***spreading co-efficient*** falls within the upper and lower limits of the predicted scenarios, closer to the lower values associated from the multiple layer scenarios.

The main knowledge gap in 1996 was with regard to the properties of the intra-reservoir mudstones, so it was not known whether the plume would form as a single CO_2 layer, at the top or at some other level within the reservoir, or as a multi-layer feature spanning much of the reservoir thickness. Consequently there was a very wide variation in predicted performance measures, particularly with respect to the development of the topmost CO_2 layer. It is notable though that the observed data do fall within the predicted limits for all of the performance measures. This is a positive result and provided a robust basis for building more informed model scenarios based on the monitoring datasets acquired from 1999 onwards.

2001 model: predictions based on baseline data plus 1999 and 2001 monitoring datasets

The time-lapse seismic monitoring surveys became available between 1999 and 2001 and immediately revealed the nature of the CO_2 plume in the reservoir (Fig. 3). The 1999 data showed the plume to comprise a number of separate reflective horizons interpreted as thin layers of CO_2 trapped beneath the intra-reservoir mudstones. Crucially, the 2001 data were able to confirm the same distinct reflections, substantiating the hypothesis of a stable plume structure with discrete and mappable spreading layers.

An additional key observation is that CO_2 reached the top of the reservoir just prior to the 1999 survey. Back-projecting the observed growth of the topmost layer by 2001 gives an arrival time at top reservoir some ten weeks before the 1999 survey. This is an important and very robust observation because it precisely defines the gross vertical flow properties of the reservoir from the injection point to the topseal.

No additional information on reservoir temperatures was available in 2001.

The key impact from the time-lapse seismics is that model scenarios with permeable and impermeable intra-reservoir mudstones were discarded. All 2001 models have semi-permeable mudstones with multi-layer plumes (Fig. 12), and mudstone effective flow properties calibrated by the observed arrival time of the CO_2 at top reservoir.

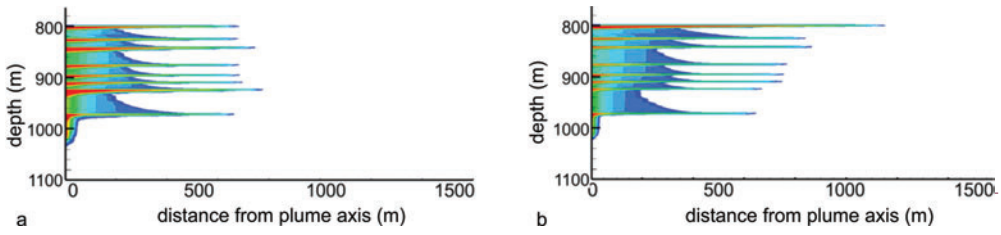

Figure 12. Predicted plume development for 2008 for the multi-layer plume, based on information available in 2001. (a) 'Low-mobility' scenario with a cool-reservoir and low permeability (1 darcy sands). (b) 'High-mobility' scenario with a warm-reservoir and higher permeability (3 darcy sands).

Development of the topmost CO_2 layer was also much better constrained by 2001, largely because the extreme limits on the amount of CO_2 reaching the reservoir top were removed (Fig. 13). 3D model end-members are controlled essentially by the range in sand permeability and reservoir temperature, both of which control plume mobility, and also by a range in the amount of CO_2 reaching the reservoir top. It is notable however that the high mobility end-member does not properly match the lateral spread of the observed data.

Overall, uncertainties in the performance measures were much reduced from the 1996 predictions (Fig. 14), summarized below:

The observed *plume footprint area* is within the predicted range, which is much tighter than for the 1996 scenarios.

Observed *lateral migration distance from the injection point* lies within the predicted range for the axisymmetric models. To achieve this did require a corrective 'eccentricity factor' to be applied, based on the observed elliptical plume geometry in plan view (Fig. 3), rather than the axisymmetric (circular) geometry of the models. The 3D models do not reproduce the maximum migration distance very well, indicating that parameter uncertainties still exist.

The observed *area of the CO_2 accumulation trapped at top reservoir* lies within the predicted limits for both axisymmetric and 3D modeling scenarios. The former still tend to give higher values than observed due to unfettered spreading beneath a flat topseal. The latter quite closely bracket the observed values suggesting some real reduction in parameter uncertainty compared with 1996.

The observed *volume of the CO_2 accumulation trapped at top reservoir* is a key parameter. It is bracketed by the predicted limits which are much tighter than in 1996. It is notable that the low mobility end-member fits the observations best, whereas the

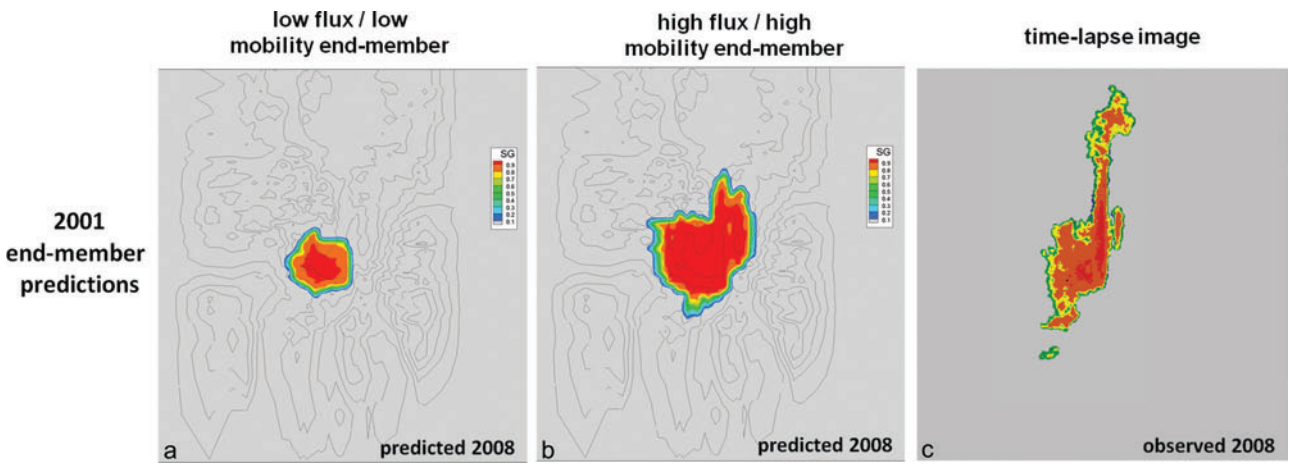

Figure 13. (a) and (b) Predictive 3D flow models of topmost layer development by 2008 based on information available in 2001, compared (c) with actual monitoring data acquired in 2008 (c).

| *Greenhouse Gas Sci Technol.* **5**:305–322 (2015); DOI: 10.1002/ghg

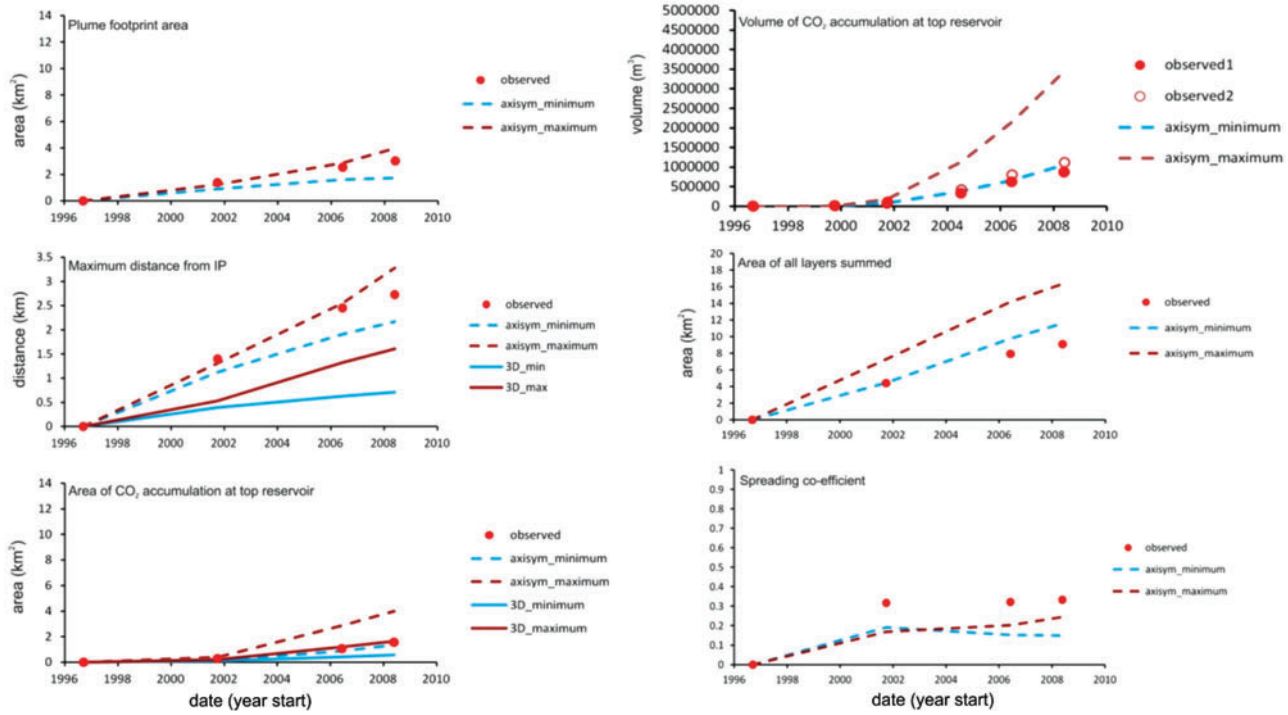

Figure 14. Summary synthesis plots for the performance measures from 2001 showing the minimum and maximum end-members of the model predictions and the observed data (red spots). Topmost layer volumes are estimated from the seismic data using two different methods.[11]

previous performance measures tend to be fitted better by the high mobility end-member. This suggests that we are not seeing a simple convergence of understanding on all modeling parameters.

The observed *area of all layers summed* falls slightly below the predicted range. This is almost certainly because the axisymmetric model allows unfettered lateral spreading beneath flat intra-reservoir seals whereas in the real reservoir buoyant ponding beneath mudstone relief will inhibit lateral spread.

The observed *spreading co-efficient* lies above the upper predicted limit, but the stability of the overall plume architecture is well reproduced by the models. There is some weak indication that the cooler (low mobility) models maintain the stable value rather better than the warmer (high mobility) scenarios.

2006 model: predictions based on baseline data plus 1999, 2001, and 2006 monitoring datasets and temperature information

In the period 2001 to 2006 additional time-lapse seismic monitoring surveys showed that the CO_2 layers established by the 1999 and 2001 surveys continued to develop in a systematic way (Fig. 3). A key additional piece of information was reservoir temperature data provided by the water production operation at the nearby Volve field [15] which confirmed a 'cool reservoir' scenario with a top reservoir temperature of 29 °C and an injection point temperature of 36 °C. [N.B. Volve operations did not actually commence until 2007, but for the purposes of this analysis we assumed that the information was available in time for the 2006 predictive scenarios]. 2006 predictive modeling therefore included only the cool reservoir scenarios (Fig. 15).

Mudstone permeabilities were further tuned to match the CO_2 arrival time at top reservoir and also the observed growth of the topmost layer. The latter spans the period from 1999 to 2006 and enables quantification of the time-variant CO_2 flux through the plume, enabling refinement of the permeability characteristics in the reservoir. An additional conformance criterion was also tested, the relative areas of the individual layers, which were matched to the monitoring data by adjusting the permeabilities of each inter-mudstone sand unit (Fig. 15). It is clear that

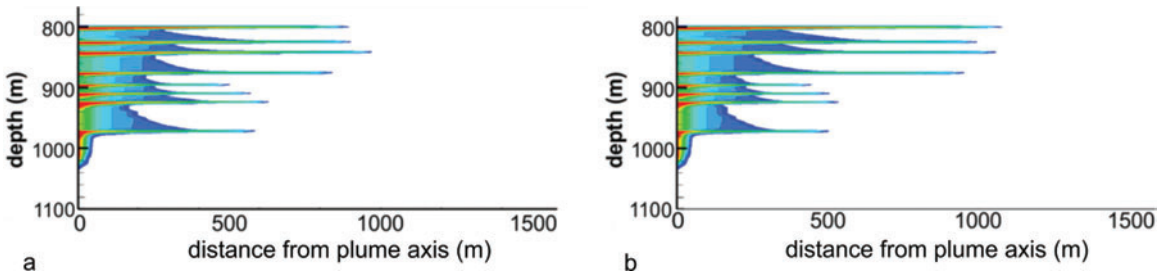

Figure 15. Predicted plume for 2008 based on information available in 2006 (a) 'Lower mobility' scenario (1 and 3 darcy sands); (b) 'Higher-mobility' scenario (1 and 6 darcy sands).

this additional conformance criterion could provide important additional insights into the reservoir permeability structure and the growth of individual layers, but details of this are outside the scope of this paper.

Prediction of the topmost CO_2 layer development continued to improve, mainly because of improved calibration of topmost layer growth, and elimination of the warm reservoir scenarios (Fig. 16). Layer growth is controlled by the uppermost sand permeability and also by the range in the amount of CO_2 reaching the reservoir top, governed by the permeability structure in the deeper reservoir. It is notable that the high mobility end-member still does not fully match the lateral spread of the observed data. This reflects residual uncertainties in terms of reservoir permeability, and the CO_2 mobility. Unlike the earlier simulations which assumed laterally uniform and isotropic permeabilities, some of the 2006 3D models followed [11] in introducing permeability anisotropy to improve matching of the lateral spread. Regarding CO_2 mobility, all the presented simulations assumed injection at reservoir temperature, but recent work[15] suggests that CO_2 in the plume might be warmer than the surrounding reservoir due to adiabatic compression and heating in the wellbore. These permeability and mobility issues would be a target for further more detailed modeling.

Overall, uncertainty in the performance measures is further reduced compared with 2001 (Fig. 17), summarized below:

The observed *plume footprint area* is within the predicted range, which is much tighter than the 1996 and significantly tighter than the 2001 scenarios. It is notable that the axisymmetric model geometry is still able to accurately predict plume footprint even with large amounts of CO_2 in the plume and the observed eccentric lateral spread of some of the layers. Plume footprint is a function of the number of layers and reservoir architecture, and its accurate prediction

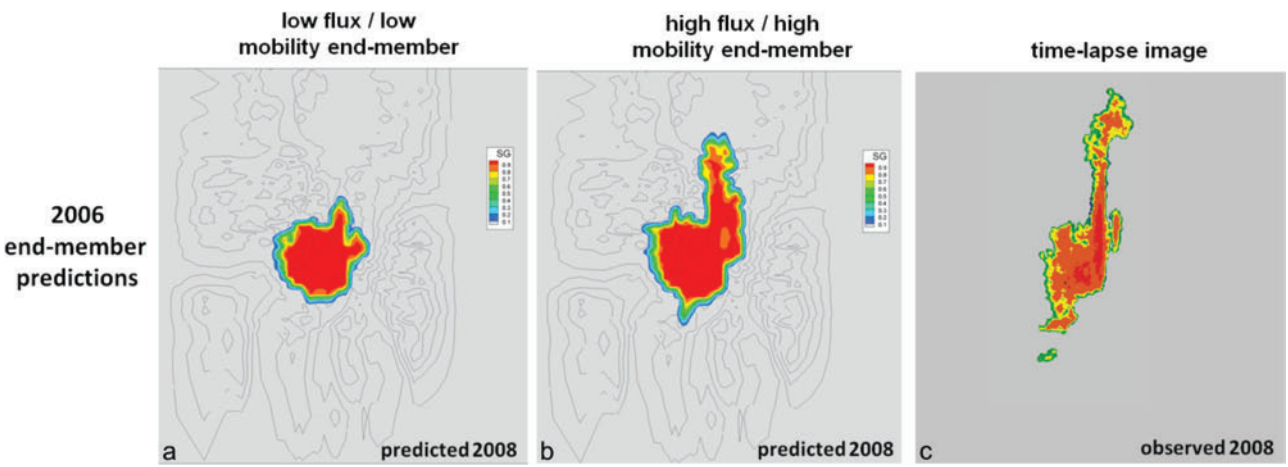

Figure 16. (a) and (b) Predictive flow models of topmost layer development by 2008 based on information available in 2006, compared with (c) actual monitoring data acquired in 2008.

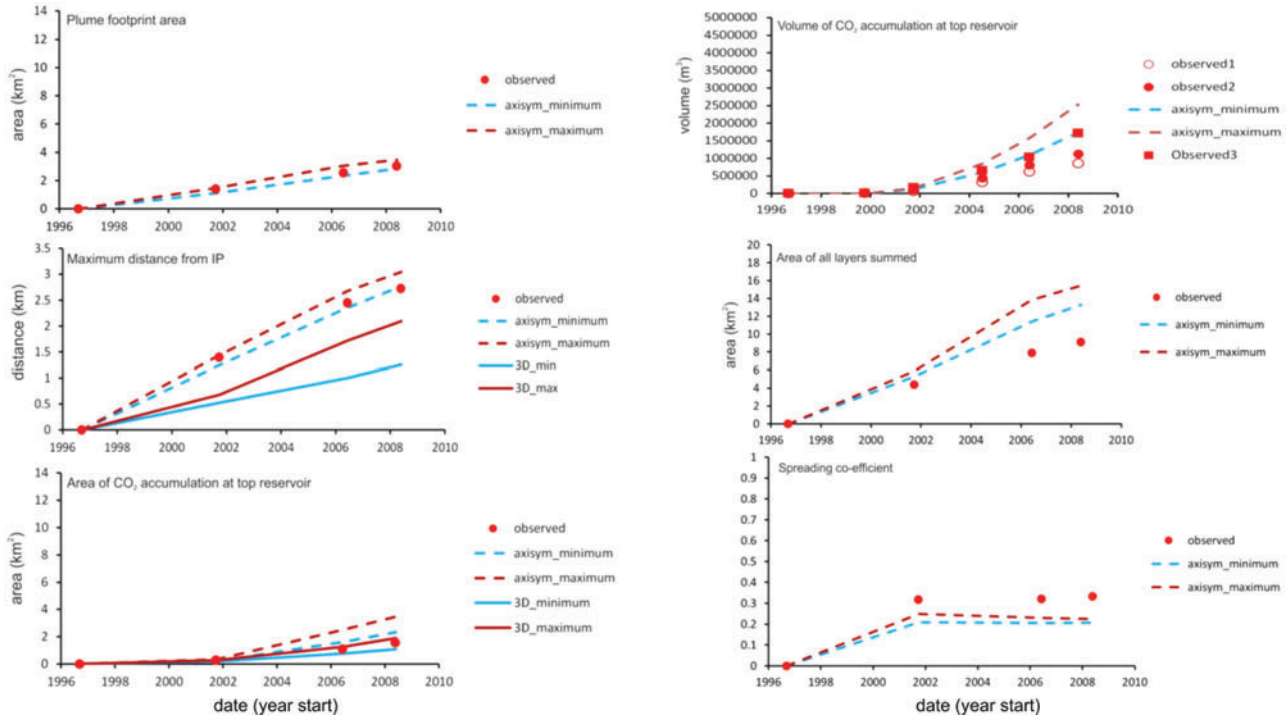

Figure 17. Summary synthesis plots for the performance measures for 2006 showing the minimum and maximum limits of the model predictions and the observed data (red spots). Topmost layer volumes are estimated from the seismic data using three different methods.

indicates that the flat-lying geometry of the axisymmetric model is generally appropriate.

Observed *lateral migration distance from the injection point* lies within the predicted range for the axisymmetric models but this is not surprising given that a corrective 'eccentricity factor' has been applied. The 3D models do not reproduce the maximum migration distance very well, but predictions are much improved on the earlier scenarios. It is clear that parameter uncertainties are still associated with the extremely rapid northward migration of the CO_2 along the linear tongue (Fig. 3), but overall the predictive ability of the 3D models is quite satisfactory.

The observed *area of the CO_2 accumulation trapped at top reservoir* lies within the predicted limits for the 3D modeling scenarios, but not for the axisymmetric ones. The former are tight and show good forward prediction to 2008, superior to the predictive capability of the 2001 3D scenarios. With the axisymmetric scenarios, the combination of the high permeabilities required at top reservoir and the flat topseal geometry of the model means that the modeled layer inevitably spreads too thinly compared with the actual layer ponded beneath topography and so has a larger spread.

The observed *volume of the CO_2 accumulation trapped at top reservoir* is a key parameter. With availability of the 2006 dataset, a third methodology was used to calculate the layer volume from the seismic data, to give three modeled values in total. For the revised calculated values it is just bracketed by the predicted limits which are much tighter than those from 1996 and significantly tighter than those from 2001. There is a tension between the need for very high permeabilities in the topmost sand (to address the observed rapid layer spread) and the observed volume of the topmost layer which is less than predicted by the axisymmetric models with a high permeability topmost layer. The prediction for 2008 is nevertheless satisfactory with observed values tracking the lower limit of the predicted range.

The observed *area of all layers summed* falls below the predicted range. This is partly because the range of the predicted values is smaller than with the earlier scenarios due to the restricted number of models run in 2006. Nevertheless, it seems that this particular performance measure cannot be reliably predicted

with the applied modeling strategy. This is almost certainly because the axisymmetric model allows unfettered lateral spreading beneath flat intra-reservoir seals whereas in the real reservoir, buoyant ponding beneath mudstone relief will inhibit lateral spread.

The observed *spreading co-efficient* lies above the upper predicted limit, but the temporal stability of the overall plume architecture is well reproduced by the models. Predicted values are between about 60% and 80% of the observed values, a notably better fit than the 2001 predictions which were typically 50– 60% for the cool reservoir (Fig. 14).

Discussion

The extensive conformance modeling exercise has demonstrated that time-lapse seismic and other monitoring data have served to radically improve understanding of plume evolution with time and our ability to make reliable predictions of future behavior (Fig. 18). Predictive models in 1996 included a wide range of plume geometries and layer configurations, with great uncertainty on predicted outcomes. The 2001 predictions had a much lower uncertainty range, based principally around the elimination of single layer plume scenarios. The 2006 predictions further improved as the 'warm' reservoir scenarios were eliminated and more details on CO_2 layer growth became available.

It is clear that even by 2006, a perfect prediction of the 2008 topmost layer was not easily obtainable. This is due to continued (though much reduced) geological uncertainty and also to likely limitations in the rather simple predictive model itself. So, as more detailed information becomes available, new areas of uncertainty arise as 'unknown unknowns' become 'known unknowns'. Nevertheless, it is also clear that the basic process of layer development (buoyancy-driven migration by fill-spill beneath the topseal topography) is satisfactorily understood and it seems clear that the new uncertainties are matters of detail that will not lead to significant unexpected future behavior.

Conclusions

Demonstrating conformance between predictive models of reservoir performance is technically challenging because a unique and perfect match is near impossible to achieve.

This study does not set out to show that the Sleipner storage site *per se* is in conformance, but rather to

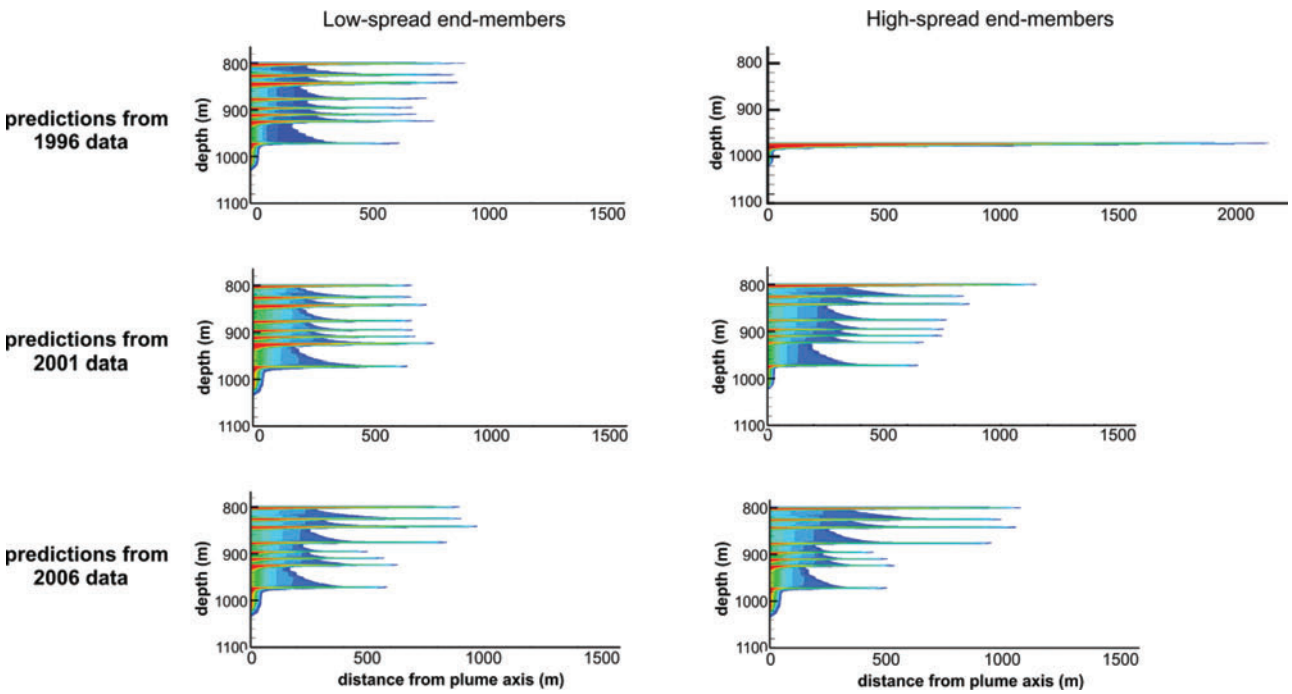

Figure 18. Predicted plumes for 2008, showing low-mobility and high mobility end-members based on 1996, 2001, and 2006 information.

illustrate a generic approach by which conformance might be demonstrated. It has shown that a set of relatively simple performance measures can be used to demonstrate storage conformance, the key element being to show that as more monitoring data is acquired through time, uncertainties progressively reduce and predictive capabilities improve. This is consistent with the underlying processes controlling plume development being understood.

As uncertainties reduce, predictive capability improves, but strong focus should still be maintained on the less likely 'end-member' model scenarios to avoid the possibility of unexpected or divergent future outcomes.

At site closure, predictive models should be sufficiently robust, and uncertainties sufficiently understood, to effectively rule out the possibility of significant adverse future outcomes.

Given the difficulty in obtaining unique or perfect matches between modeled and observed data it is recommended that regulators set conformance criteria at realistic achievable levels, focussing principally on progressive reduction of uncertainty with time and demonstration that the fundamental storage processes are sufficiently well understood.

Acknowledgements

This paper is published with permission of the Executive Director British Geological Survey (NERC). The work was carried out within the CO2CARE project which is funded by the European Commission within the 7th Framework Programme and also co-financed by an industrial consortium of RWE, Shell, Statoil, TOTAL, Vattenfall and Veolia. The financial support of the EC and the industry partners is greatly appreciated.

References

1. European Commission, *Implementation of Directive 2009/31/EC on the Geological Storage of Carbon Dioxide. Guidance Document 2: Characterisation of the Storage Complex, CO_2 Stream Composition, Monitoring and Corrective Measures*. EC, Brussels (2011).
2. Korbøl R and Kaddour A, Sleipner vest CO_2 disposal – injection of removed CO_2 into the Utsira Formation, *Energy Conversion and Management*, **36**:509–512.
3. Baklid A, Korbøl R and Owren G, *Sleipner vest CO_2 disposal, CO_2 injection into a shallow underground aquifer.* SPE paper 36600, *1996 SPE Annual Technical Conference and Exhibition*, Denver, CO, USA, 6–9 October (1996).
4. Zweigel P, Arts R, Lothe AE and Lindeberg ERG, Reservoir geology of the Utsira Formation at the first industrial-scale underground CO_2 storage site (Sleipner area, North Sea), in *Geological Storage for CO_2 Emissions Reduction*, ed by Baines S , Gale J and Worden RJ, *Sp Publ Geol Soc* **233**:165–180 (2004).
5. Chadwick RA, Zweigel P, Gregersen U, Kirby GA, Johannessen PN and Holloway S, Characterisation of a CO_2 storage site: The Utsira Sand, Sleipner, northern North Sea. *Energy* **29**:1371–1381(2004).
6. Zweigel P, Hamborg M, Arts R, Lothe AE, Sylta O and Tommeras A, Prediction of migration of CO_2 injected into an underground depository: Reservoir geology and migration modelling in the Sleipner case (North Sea), in *Greenhouse Gas Control Technologies, Proceedings of the 5th International Conference on Greenhouse Gas Control Technologies*, 13–16 August 2000, ed by Williams D, Durie I, McMullan P, Paulson C and Smith A. CSIRO, Cairns, Australia, pp. 360–365 (2001).
7. Harrington JF, Noy DJ, Horseman ST, Birchall DJ and Chadwick RA, Laboratory study of gas and water flow in the Nordland Shale, Sleipner, North Sea, in *Carbon Dioxide Sequestration in Geological Media – State of the science*, ed by Grobe M, Pashin J and Dodge R. *AAPG Stud Geol* **59**:521–543 (2010).
8. Arts RJ, Chadwick RA, Eiken O, Dortland S, Trani M and Van Der Meer LGH, Acoustic and elastic modelling of seismic time-lapse data from the Sleipner CO_2 storage operation, in *Carbon Dioxide Sequestration in Geological Media – State of the Science*, ed by Grobe M, Pashin J and Dodge R. *AAPG Stud Geol* **59**:391–403 (2010).
9. Arts RJ, Eiken O, Chadwick RA, Zweigel P, Van Der Meer L and Zinszner B, Monitoring of CO_2 injected at Sleipner using time-lapse seismic data. *Energy* **29**:1383–1393 (2004).
10. Chadwick RA, Arts R, Eiken O, Kirby GA, Lindeberg E and Zweigel P, 4D seismic imaging of an injected CO_2 bubble at the Sleipner Field, central North Sea, in *3-D Seismic Technology: Application to the Exploration of Sedimentary Basins,* Memoir no. 29, ed by DaviesRJ , Cartwright JA, Stewart SA, Lappin M and Underhill JR. Geological Society, London, pp. 305–314 (2004).
11. Chadwick RA and Noy DJ. History – matching flow simulations and time-lapse seismic data from the Sleipner CO_2 plume, in *Petroleum Geology: From Mature basins to New Frontiers – Proceedings of the 7th Petroleum Geology Conference*, ed by Vining BA and Pickering SC. Geological Society, London, pp. 1171–1182 (2010).
12. Cavanagh AJ, Benchmark calibration and prediction of the Sleipner CO_2 plume from 2006 to 2012. *Energ Procedia* **37**:3529–3545 (2013).
13. Pruess K, Oldenburg C and Moridis G, *TOUGH2 User Guide, version 2.0.* Report LBNL-43134, Lawrence Berkeley National Laboratory, Berkeley, CA, USA (1999).
14. Pruess K, *ECO2N: A TOUGH2 Fluid Property Module for Mixtures of Water, NaCl, and CO_2,* Report LBNL-57952. Lawrence Berkeley National Laboratory, Berkeley, CA, USA (2005).
15. Alnes H, Eiken O, Nooner S, Sasagawa G, Stenvold T, Zumberge M. Results from Sleipner gravity monitoring: Updated density and temperature distribution of the CO_2 plume. Proceedings of the GHGT-10 Conference. *Energ Procedia* **4**:5504–5511 (2011).

R. Andrew Chadwick

R. Andrew Chadwick is an Individual Merit Research Scientist at BGS. He has more than 30 years' experience in subsurface geology, basin evolution and seismic analysis. His CCS interests lie in site characterisation and monitoring, including integrated analysis of time-lapse seismics and reservoir flow modelling to understand CO_2 storage processes.

David J. Noy

David J. Noy is a physicist with more than 30 years' research into groundwater flow and contaminants migration, including modelling gas migration in porous media, and osmotic effects in argillaceous rocks. He has a particular focus on coupled processes such as reactive multicomponent transport, density dependent groundwater flow, and CO_2 storage.

| *Greenhouse Gas Sci Technol.* **5**:305–322 (2015); DOI: 10.1002/ghg